HIGH TECHNOLOGY LETTERS | Vol. 29 No. 1 | Mar. 2023 | pp. 105-112

doi:10.3772/j.issn.1006-6748.2023.01.012

Design and analysis of a two-dimensional vibration control mechanism based on vibro-impact damping①

ZHANG Laixi(张来喜), QIAN Feng, WU Mingliang②
(School of Mechanical and Electronical Engineering, Lanzhou University of Technology, Lanzhou 730050, P. R. China)

Abstract

The robotic drilling always generates the axial vibration along the drill bit and the torsional vibration around the drill bit, which will adversely affect the drilling precision. A vibration control mechanism fixed between the end-effector and the robot is proposed, which can suppress the axial and torsional vibrations based on the principle of vibro-impact (VI) damping. The energy dissipation of the system by vibro-impact damping is analyzed. Then, the influence of the structure parameters on the vibration attenuation effect is studied, and a semi-active vibration control method of variable collision clearance is presented. The simulation results show that the control method has effective vibration control performance.

Key words: robotic drilling, two-dimensional vibration control, impact damping, variable clearance, semi-active vibration control

0 Introduction

Robotic drilling technology has been widely applied in aviation manufacturing field for its flexibility and adaptability, which greatly improves the efficiency and quality of automatic drilling[1]. However, due to the insufficient inherent stiffness of the industrial robot, vibration or even flutter will occur under special working conditions, affecting the precision of robotic drilling[2]. Meanwhile, there exists thin-wall vibration in robotic drilling due to thin-walled structure of the aircraft skin, and the vibration will be transmitted to the end-effector through the drill bit[3], and then to the robot through the end-effector, which will also adversely affect the drilling accuracy. Vibration isolation, dynamic vibration absorption, impact damping and other methods are used to control the harmful vibration. Among them, the impact absorber has attracted extensive research by researchers because of its simple structure, wide frequency band and stable damping effect. Impact absorbers transfer and dissipate vibration energy from the main vibration system through collision, and are widely used in construction and mechanical fields[4]. Ref. [5] added an impact absorber on the basis of the nonlinear energy sink structure, proved that the impact absorber and the nonlinear energy sink (NES) coupling system have better vibration suppression performance. Ref. [6] established a cantilever beam model with an impact damper, and the impact damper can effectively suppress multiple resonance peaks of the cantilever beam. Ref. [4] analyzed the dissipation mechanism of structural vibration energy caused by impact absorber, and revealed the transfer and diffusion law of vibration energy in various modes of the system at the moment of collision. Refs [7,8] studied the vibration control performance of a pounding tuned rotary mass damper (PTRMD) placed inside the cavity floor, and the results showed that the structure had good vibration attenuation performance under free vibration, harmonic excitation and earthquake excitation. In addition, the introduction of impact collision based on the original vibration reduction method can further improve the vibration suppression performance. Ref. [9] used a pounding tuned mass damper for controlling the structural vibration of a monopile offshore wind turbines subjected to combined wind and wave loading. Research suggests that the introduced collision mechanism improves the robustness of the tuned mass damper with enhanced vibration control effect under the detuned situations. Ref. [10] proposed a particle impact damped dynamic absorber and compared it with the classical dynamic absorber. Experimental results show that the particle impact damped dynamic absorber expands the working frequency range and exhibits a better random vibration suppression performance than

① Supported by the National Natural Science Foundation of China (No. 52265013) and Natural Science Foundation of Gansu Province (No. 20JR5RA457).
② To whom correspondence should be addressed. E-mail: wlm0757@163.com.
Received on Jan. 26, 2022

the classical dynamic absorber.

Ref. [11] proposed an adaptive control strategy for torsional vibration of the main drive system of rolling mill, which effectively suppressed the torsional vibration of the system. In order to reduce the influence of torsional vibration generated by the drivetrain on vehicle ride comfort, Ref. [12] combined the torsional vibration isolator and vibration absorber into the vehicle drivetrain and proposed a frequency tuning control scheme, which effectively reduced the torsional vibration generated by the drivetrain. Ref. [13] found that NES impact absorbers can significantly suppress the torsional vibration not only far from and close to resonance, but also in a wide frequency range. Ref. [14] designed a nonlinear torsional vibration isolator of a parallel mechanism with positive and negative stiffness to solve the problem of low-frequency torsional micro-vibration. The torsional vibration isolator can adapt to complex and variable loads and interference torque, and has good anti-disturbance ability and vibration isolation performance. In Refs[15,16], a semi-active vibration control mechanism was designed based on quasi-zero stiffness for robotic drilling system to suppression the ambient vibration.

The research on vibration control has been relatively mature, but most of them only solve the vibration in one direction. However, in practice, axial vibration and torsional vibration often occur simultaneously. Ref. [17] effectively controlled the axial and torsional vibrations of the engine system with impact absorber of controllable frequency and damping to transfer vibration energy through modal interaction with the engine system and internal resonance.

A two-dimensional integrated vibration control device based on variable parameters of vibro-impact damping is proposed to suppress the axial and torsional vibration simultaneously.

1 Structure of the vibration control mechanism

The robotic drilling system equipped with vibration control mechanism is shown in Fig. 1. This paper designs a vibration control mechanism fixed between the robot and the end-effector, which transfers and dissipates the vibration energy with the principle of vibro-impact damping to restrain the axial and torsional vibrations from the end-effector, and improves the drilling precision.

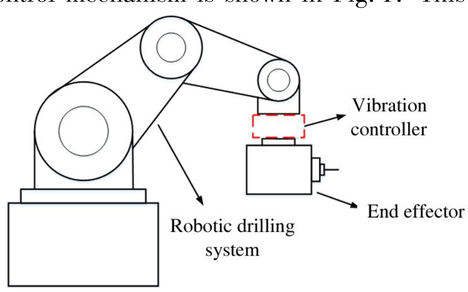

Fig. 1 Robotic drilling system with vibration control mechanism

The vibration control mechanism consists of two parts: axial control structure and torsion control structure. As shown in Fig. 2, the axial control part is composed of moving slider, impact vibrator, three-jaw fixed slider, coupling, servo motor, ball screw and rotating ball spline. The axial control part drives the dynamic slider to move along the axial direction of the ball screw to achieve the adjustment of axial collision clearance. The torsion control part is composed of impact vibrator, three-jaw fixed slider, three-jaw retaining ring, flat key shaft, worm, worm gear, coupling and servo motor. By twisting the control part to drive the rotation of the three-jaw retaining ring, the relative rotation angle between the three-jaw retaining ring and the three-jaw fixed slider can be adjusted to achieve the configuration of collision angular clearance.

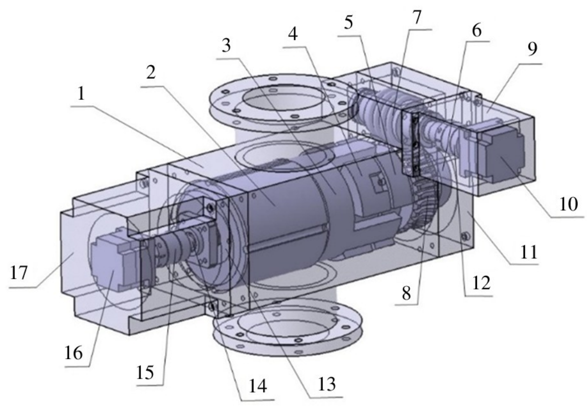

1. shell 2. moving slider 3. impact vibrator 4. three-jaw fixed slider 5. three-jaw retaining ring 6. flat key shaft 7. worm 8. worm gear 9. side cover 10. servo motor 11. rear cover 12. coupling 13. rotating ball spline 14. ball screw 15. coupling 16. servo motor 17. front cover

Fig. 2 The two-dimensional integral vibration control mechanism

2 Dynamic model

2.1 Axial dynamic model

The axial model of robotic drilling system equipped with vibration controller is shown in Fig. 3, where, the mass of the robot is m_1, the mass of the main structure of the vibration control mechanism is m_2, the mass of the end-effector is m_3, and the mass of the impact vibrator is m_4. The equivalent stiffness and damping of the robot are k_1 and c_1 respectively. The equivalent stiffness and damping between m_2 and m_1 are k_2 and c_2 respectively. The equivalent stiffness and damping between m_3 and m_2 are k_3 and c_3 respectively.

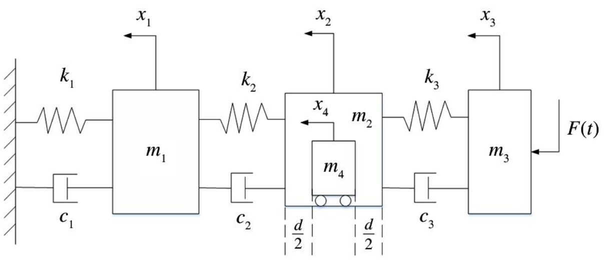

Fig. 3 The axial model of the robotic drilling system

During robotic drilling, the end-effector will be subjected to axial force along the drill bit. Assuming that m_3 is subjected to a simple harmonic excitation force of $F(t) = F\cos(\omega_1 t)$, inelastic collision will occur in the impact vibrator at this moment, resulting in the abrupt change of the velocity of m_2 and m_4, which can dissipate part of the energy of the main vibration system, thus reducing the vibration generated by the system. The whole system becomes nonlinear at the moment of collision. Except for the moment of collision, the whole system is still a linear system, which satisfies the linear vibration theory. At this time, the system dynamic equation is

$$\begin{cases} m_1\ddot{x}_1 + c_1\dot{x}_1 + k_1x_1 + c_2(0\dot{x}_1 - \dot{x}_2) + k_2(x_1 - x_2) = 0 \\ m_2\ddot{x}_2 + c_2(\dot{x}_2 - \dot{x}_1) + k_2(x_2 - x_1) + c_3(\dot{x}_2 - \dot{x}_3) \\ \qquad + k_3(x_2 - x_3) = 0 \\ m_3\ddot{x}_3 + c_3(\dot{x}_3 - \dot{x}_2) + k_3(x_3 - x_2) = F(t) \\ m_4\ddot{x}_4 = 0 \end{cases} \tag{1}$$

Assuming that the initial position of the impact vibrator is in the middle of the main structure of the vibration control mechanism and at the moment of collision, the relative displacement of m_2 and m_4 should meet the following conditions:

$$| x_2 - x_4 | = \frac{d}{2} \tag{2}$$

where x_2 is the displacement of the main structure of the vibration control mechanism, x_4 is the displacement of the impact vibrator, and d is the collision clearance.

When the collision occurs, the instantaneous displacement of m_2 and m_4 remains unchanged, but their instantaneous velocity will vary and is expressed as

$$e_1 = -\frac{\dot{x}_4^+ - \dot{x}_2^+}{\dot{x}_4 - \dot{x}_2} \tag{3}$$

where e_1 is the collision recovery coefficient, $\dot{x}_i$ and $\dot{x}_i^+$ represent the instantaneous velocities before and after the collision.

In the collision process, the system satisfies momentum conservation law:

$$m_2\dot{x}_2 + m_4\dot{x}_4 = m_2\dot{x}_2^+ + m_4\dot{x}_4^+ \tag{4}$$

By combining Eqs(3) and (4), the instantaneous velocity after the collision between m_2 and m_4 can be obtained as

$$\begin{cases} \dot{x}_2^+ = \dfrac{m_2 - m_4e_1}{m_2 + m_4}\dot{x}_2 + \dfrac{m_4(1 + e_1)}{m_2 + m_4}\dot{x}_4 \\ \dot{x}_4^+ = \dfrac{m_2(1 + e_1)}{m_2 + m_4}\dot{x}_2 + \dfrac{m_4 - m_2e_1}{m_2 + m_4}\dot{x}_4 \end{cases} \tag{5}$$

2.2 Torsional dynamic model

The torsional dynamic model is shown in Fig. 4, and the internal section diagram of the vibration control mechanism is shown in Fig. 5, where the rotational inertias of the robot, the main structure, the end-effector and the shock vibrator are J_1, J_2, J_3, and J_4, respectively. The equivalent torsional stiffness and damping of the robot are k_1' and c'_1, respectively. The equivalent torsional stiffness and damping between J_1 and J_2 are k'_2 and c'_2, respectively. The equivalent torsional stiffness and damping between J_2 and J_3 are k'_3 and c'_3 respectively.

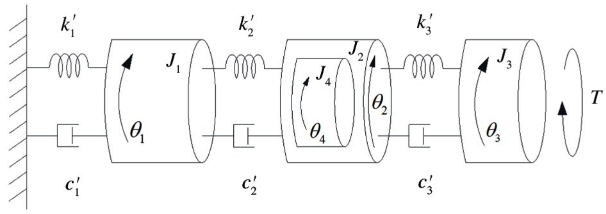

Fig. 4 The torsional model of the robotic drilling system

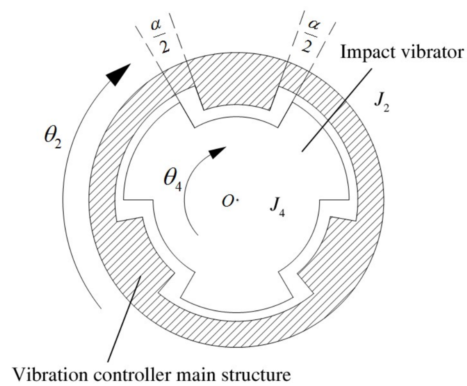

Fig. 5 The internal section diagram of the vibration control mechanism

In robotic drilling, the end-effector is excited by friction torque between the high-speed rotating drill bit and workpiece. It is assumed that the simple harmonic excitation torque is $T(t) = T\cos(\omega_2 t)$, where T represents excitation amplitude and ω_2 is excitation frequency. As shown in Fig. 5, under the excitation torque, the impact vibrator rotates around the axis O and inelastic collision occurs inside the vibration control mechanism. Thus, part of the energy can be transferred and consumed, and the torsional vibration can be suppressed. Except for the moment of collision, the whole system is still a linear system, which satisfies the linear vibration theory. Therefore, the torsional dynamic equation is established as follows.

$$\begin{cases} J_1\ddot{\theta}_1 + c_1'\dot{\theta}_1 + k_1'\theta_1 + c_2'(\dot{\theta}_1 - \dot{\theta}_2) + k_2'(\theta_1 - \theta_2) = 0 \\ J_2\ddot{\theta}_2 + c_2'(\dot{\theta}_2 - \dot{\theta}_1) + k_2'(\theta_2 - \theta_1) + c_3'(\dot{\theta}_2 - \dot{\theta}_3) \\ \qquad + k_3'(\theta_2 - \theta_3) = 0 \\ J_3\ddot{\theta}_3 + c_3'(\dot{\theta}_3 - \dot{\theta}_2) + k_3'(\theta_3 - \theta_2) = T(t) \\ J_4\ddot{\theta}_4 = 0 \end{cases} \tag{6}$$

Assuming that the initial rotation position of the impact vibrator is symmetric at the center of the vibration control mechanism, the relative angular displacement of J_2 and J_4 should meet the following conditions at the moment of collision.

$$| \theta_2 - \theta_4 | = \frac{\alpha}{2} \tag{7}$$

where θ_2 and θ_4 are the angular displacements of the main structure and the impact vibrator, respectively, and α is the angle of impact.

In collision, the instantaneous angular displacements of J_2 and J_4 remain unchanged, but the instantaneous angular velocities vary, which are expressed as

$$e_2 = -\frac{\dot{\theta}_4^+ - \dot{\theta}_2^+}{\dot{\theta}_4 - \dot{\theta}_2} \tag{8}$$

where e_2 is the collision recovery coefficient, and $\dot{\theta}_i$ and $\dot{\theta}_i^+$ are instantaneous angular velocities before and after the collision, respectively.

During the collision, the system satisfies the conservation of angular momentum:

$$J_2\dot{\theta}_2 + J_4\dot{\theta}_4 = J_2\dot{\theta}_2^+ + J_4\dot{\theta}_4^+ \tag{9}$$

Combining Eq. (8) with Eq. (9), the instantaneous angular velocities after collision between J_2 and J_4 are expressed as

$$\begin{cases} \dot{\theta}_2^+ = \dfrac{J_2 - J_4 e_2}{J_2 + J_4}\dot{\theta}_2 + \dfrac{J_4(1 + e_2)}{J_2 + J_4}\dot{\theta}_4 \\ \dot{\theta}_4^+ = \dfrac{J_2(1 + e_2)}{J_2 + J_4}\dot{\theta}_2 + \dfrac{J_4 - J_2 e_2}{J_2 + J_4}\dot{\theta}_4 \end{cases} \tag{10}$$

3 Energy dissipation analysis

This paper analyzes the damping performance of the vibration control mechanism based on axial and torsional displacement responses and energy transfer dissipation. The FANUC M-710IC robot is selected as the drilling robot. According to the system structure size, the structural parameters are listed in Tables 1 and 2. The control parameters are set initially as $d = 1.7$ mm, $\alpha = 0.096$ rad, $e_1 = 0.6$, $e_2 = 0.1$, $F = 50$ N, $\omega_1 = 50$ rad/s, $T = 4$ N · m, $\omega_2 = 20$ rad/s.

Table 1 Structural parameters of the axial vibration system

Parameter	Value
m_1	560 kg
m_2	20 kg
m_3	40 kg
m_4	1.2 kg
k_1	50 000 N/m
k_2	120 000 N/m
k_3	120 000 N/m
c_1	0.1 N · s/m
c_2	0.05 N · s/m
c_3	0.05 N · s/m

Table 2 Structural parameters of the torsional vibration system

Parameter	Value
J_1	10 kg · m^2
J_2	0.5 kg · m^2
J_3	0.6 kg · m^2
J_4	0.03 kg · m^2
k_1'	3200 N · m/rad
k_2'	15 600 N · m/rad
k_3'	15 600 N · m/rad
c_1'	0.15 N · m · s/rad
c_2'	0.10 N · m · s/rad
c_3'	0.10 N · m · s/rad

In addition to damping energy consumption, the vibration control mechanism can transfer and consume vibration energy by generating impact collision through impact vibrator.

In collision between the main structure and the impact vibrator, the speeds of the two parts vary dramatically, which results in the transfer of kinetic energy between the two parts. If the impact vibrator gains a larger speed after the collision, more kinetic energy can be transferred. E_{t1} and E_{t2} represent the kinetic energy transfer caused by axial and torsional collisions, respectively. The kinetic energy transfer is expressed as follows[18].

$$E_{t1} = \frac{m_4}{2}(\dot{x}_4^{+2} - \dot{x}_4^2) \tag{11}$$

$$E_{t2} = \frac{J_4}{2}(\dot{\theta}_4^{+2} - \dot{\theta}_4^2) \tag{12}$$

Due to the viscoelasticity of the collision surface, part of the vibration energy are consumed. E_{d1} and E_{d2} represent the axial and torsional collision consumption energy. The collision consumption energy is expressed as

$$E_{d1} = \frac{m_2 m_4 (\dot{x}_2 - \dot{x}_4)^2 (1 - e_1^2)}{2(m_2 + m_4)} \tag{13}$$

$$E_{d2} = \frac{J_2 J_4 (\dot{\theta}_2 - \dot{\theta}_4)^2 (1 - e_2^2)}{2(J_2 + J_4)} \tag{14}$$

Collisions transfer and consume vibration energy, as does system damping. E_{c1} and E_{c2} are the axial and torsional damping energy dissipation, respectively, and the damping energy dissipation is depicted as

$$E_{c1} = \int_0^t [c_1 \dot{x}_1^2 + c_2 (\dot{x}_2 - \dot{x}_1)^2 + c_3 (\dot{x}_3 - \dot{x}_2)^2] \mathrm{d}t \tag{15}$$

$$E_{c2} = \int_0^t [c_1' \dot{\theta}_1^2 + c_2' (\dot{\theta}_2 - \dot{\theta}_1)^2 + c_3' (\dot{\theta}_3 - \dot{\theta}_2)^2] \mathrm{d}t \tag{16}$$

As shown in Fig. 6, the axial energy dissipation of the system with vibration control mechanism is composed of three parts: damping energy dissipation, collision energy dissipation, and the kinetic energy transfer that plays a more important role than the collision energy dissipation. Fig. 7 shows the total vibration energy consumed by the system. It can be seen that the system with vibration control mechanism consumes more vibration energy than the original system.

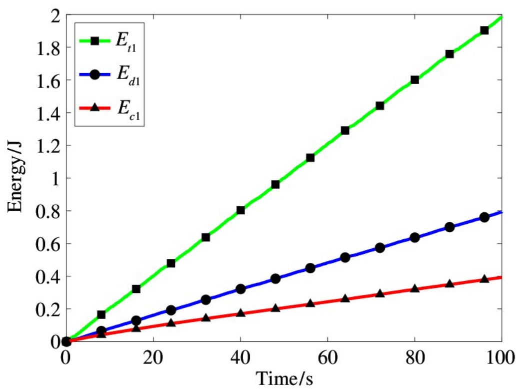

Fig. 6 Axial energy consumption

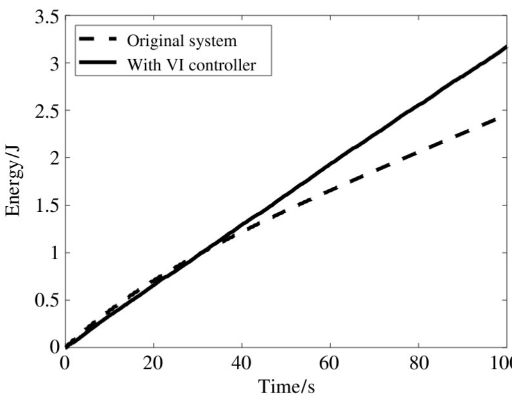

Fig. 7 Comparison of axial energy consumption

Fig. 8 shows the energy dissipation of torsional vibration. Collision dissipates a small part of the vibration energy. Kinetic energy transfer plays a more important role than collision energy dissipation.

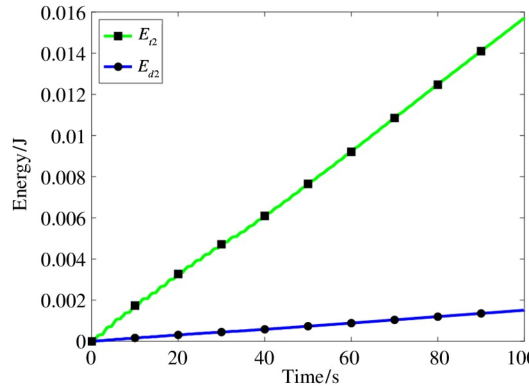

Fig. 8 Torsional energy consumption

4 Parameters analysis

The parameters of vibration control mechanism will affect the damping effect of robotic drilling system. The parameters of axial vibration mainly include impact vibrator mass m_4, collision recovery coefficient e_1 and collision clearance d. The parameters of torsional vibration are the moment of inertia of impact vibrator J_4, the collision recovery coefficient e_2 and the collision angularclearance α.

4.1 Impact vibrator mass and collision recovery coefficient

The impact vibrator mass m_4 and collision recovery coefficient e_1 will not vary once determined. The collision clearance is set as a constant variable to discuss the influence of m_4 and e_1 on vibration damping performance. As shown in Fig. 9(a), with the increase of m_4 and decrease of e_1, the response displacement decreases and the vibration damping effect is improved. Due to the nonlinearity of impact collision, some parameters vary irregularly without penalty of the overall damping law.

As shown in Fig. 9(b), the collision angular clearance α is fixed, and the moment of inertia of impact vibrator J_4 and the collision recovery coefficient e_2 are taken as variables. It can be seen that with the increase of J_4, the response angular displacement decreases. The smaller e_2 is, the response angular displacement decreases as well. It shows that a larger J_4 and a smaller e_2 is beneficial to reduce the torsional vibration of the system. In a certain range, the larger m_4 and J_4 and the smaller e_1 and e_2 are more beneficial to reduce the vibration of the system.

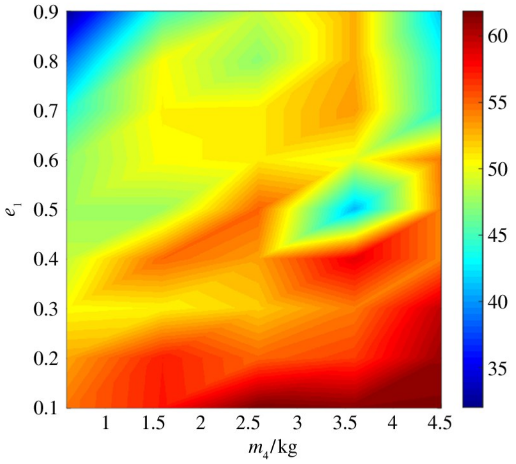

(a) Axial direction

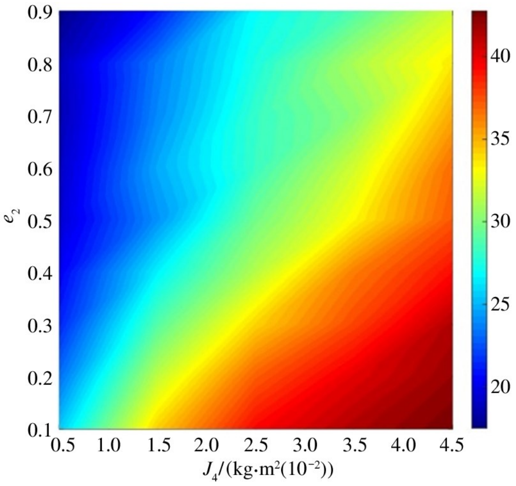

(b) Torsional direction

Fig. 9 The influence of impact vibrator and collision recovery coefficient on the damping performance

4.2 Collision clearance

In order to evaluate the impact of collision clearance d on the vibration damping performance, the response displacement suppression ratio is obtained by fixing m_4 and e_1 and varying d. The impact of collision clearance on the vibration damping performance under different excitation frequencies is analyzed.

As shown in Fig. 10(a), when the excitation frequency is 50 rad/s, within the range of effective collision clearance, the displacement suppression ratio does not show obvious law with the clearance. However, the displacement suppression ratio is the highest under the collision clearance of 0.8 mm, reaching 61.86%. Other collision also play a certain role in damping, but the displacement suppression ratio is relatively small. As shown in Fig. 10(b), when the excitation frequency is 80 rad/s, the displacement suppression ratio does not show regular law with the clearance as well. The better collision clearance is 0.18 mm and 0.20 mm, and the displacement suppression ratio is 54.2% and 54.0%, respectively. At certain collision clearance, the displacement suppression ratio worsens. Therefore, within the range of effective collision clearance, the worsening collision clearance area should be avoided and the relatively optimal collision clearance should be selected. As shown in Fig. 10(c), when the excitation frequency is 100 rad/s and the collision clearance is 0.5 mm, the displacement suppression ratio is 34.65%, and the vibration damping effect is the best. Because of the high excitation frequency, when the collision clearance is large, collision will deteriorate the vibration damping. The reason is that under high frequency excitation, the clearance is too large to have time for reaction of the impact vibrator, so it moves together with the system and generates resonance.

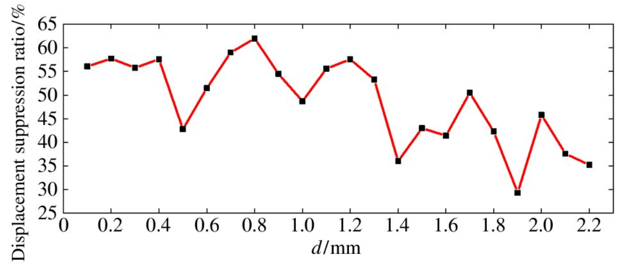

(a) 50 rad/s

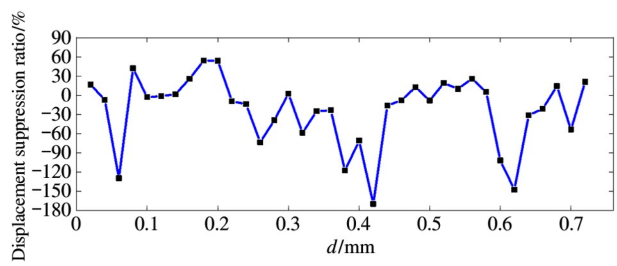

(b) 80 rad/s

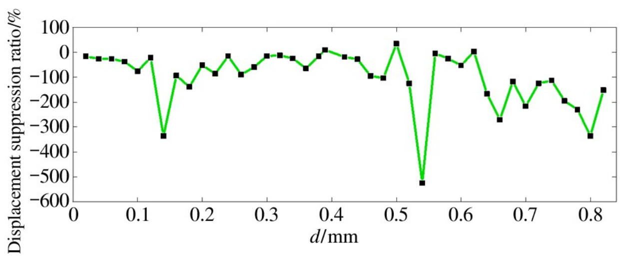

(c) 100 rad/s

Fig. 10 The impact of collision clearance on the vibration damping performance

4.3 Collision angular clearance

The influence of collision angular clearance on damping performance under different excitation frequencies is discussed, where $J_4 = 0.04\ \mathrm{kg \cdot m^2}$, $e_2 = 0.1$. As shown in Fig. 11(a), when the excitation frequency is 20 rad/s, with the increase of the collision angular clearance, the angular displacement suppression ratio gradually increases in general, and there is a few point that the angular displacement suppression ratio decreases. The angular displacement suppression ratio reaches the highest value of 42.4% where the collision angular clearance is 0.0128 rad. As shown in Fig. 11(b), when the excitation frequency is 30 rad/s, with the increase of collision angular clearance, the angular displacement suppression ratio first increases, then decreases and then increases. The highest angular displacement suppression ratio is 32.3% where the collision angular clearance is 0.0022 rad. As shown in Fig. 11(c), when the excitation frequency is 40 rad/s, the highest angular displacement suppression ratio is 28.8% where the collision angular clearance is 0.000 34 rad.

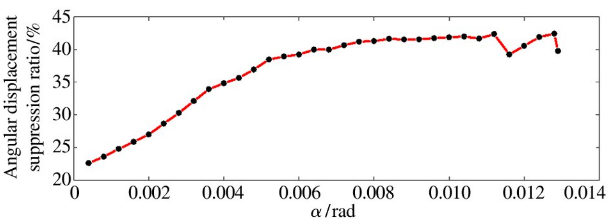

(a) 20 rad/s

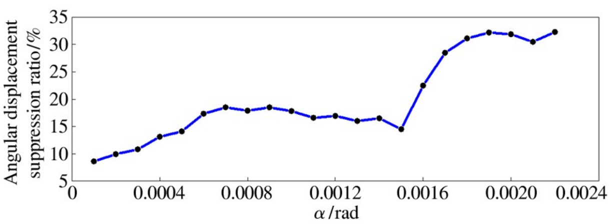

(b) 30 rad/s

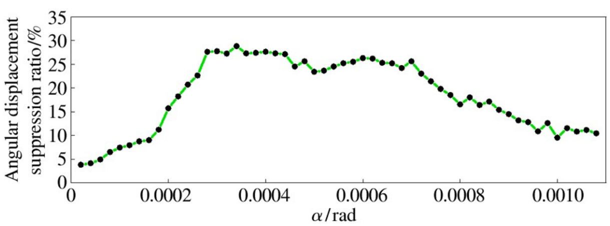

(c) 40 rad/s

Fig. 11 The impact of collision angular clearance on the vibration damping performance

In summary, within the effective collision clearance, there is no definite regular law between the vibration damping effect and the collision clearance. However, there exist some optimum collision clearances that can achieve an improved damping performance.

5 Simulation of variable clearance semi-active control

Adjusting some structural parameters could achieve active vibration control in a certain frequency range, it will constitute a semi-active vibration control system with the system in which the structural parameters could not be adjusted.

By using Matlab, a group of optimal impact vibrator mass m_4 (4 kg) and collision recovery coefficient e_1 (0.3) were configured. A segmental variable frequency excitation for simulation of the axial vibration control was designed for the semi-active control with variable collision clearance d, which is expressed as Eq. (17).

$$\begin{cases} F(t) = 50\cos(100t) & 0-60\ \text{s} \\ F(t) = 50\cos(80t) & 60-120\ \text{s} \\ F(t) = 50\cos(50t) & 120-180\ \text{s} \end{cases} \tag{17}$$

As shown in Fig. 12, the axial displacement response of the robot equipped with vibration control device is superior to that of the original system. The axial displacement suppression ratio is 34.6% under the excitation frequency of 100 rad/s. The axial displacement suppression ratio is 54.2% under the excitation frequency of 80 rad/s. The axial displacement suppression ratio is 62.0% under the excitation frequency of 50 rad/s. It is shown that the variable-clearance vibration control method proposed in this paper can adapt to the variable frequency excitations, and realize the suppression of axial vibration.

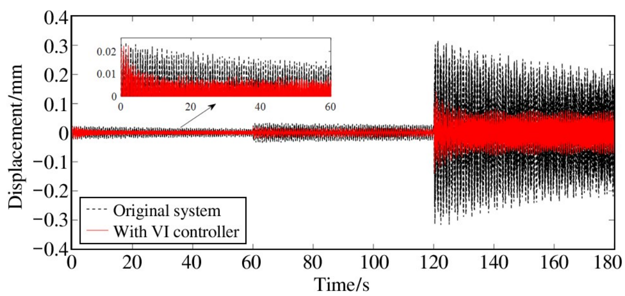

Fig. 12 Simulation of variable clearance control of axial vibration

A segmental variable frequency excitation for simulation of the torsional vibration control was designed for the semi-active control with variable collision angular clearance α, which is expressed as Eq. (18).

$$\begin{cases} T(t) = 4\cos(40t) & 0-60\ \text{s} \\ T(t) = 4\cos(30t) & 60-120\ \text{s} \\ T(t) = 4\cos(20t) & 120-180\ \text{s} \end{cases} \tag{18}$$

As shown in Fig. 13, the angular displacement response of the robot equipped with vibration control device is superior to that of the original system. The angular displacement suppression ratio is 28.8% under the excitation frequency of 40 rad/s. The angular displacement suppression ratio is 32.3% under the excitation frequency of 30 rad/s. The angular displacement suppression ratio is 42.4% under the excitation frequency of 20 rad/s. It is shown that the variable-clearance vibration control method can realize the suppression of torsional vibration as well.

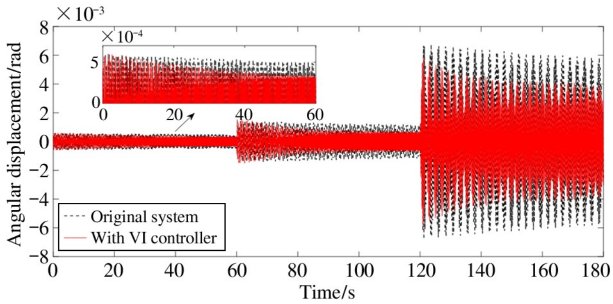

Fig. 13 Simulation of variable clearance control of torsional vibration

6 Conclusion

A two-dimensional vibration control device based on impact damping is proposed to deal with the axial vibration and torsional vibration in robotic drilling. The axial and torsional dynamic equations are established respectively, and the influence of various structural parameters on the damping performance is analyzed by collision theory and energy dissipation theory.

By adjusting the collision clearance, the displacement suppression ratio can be optimized according to the frequency of the excitations. The Matlab simulation results show that impact collision can increase the dissipation of vibration energy of the system, in which kinetic energy transfer plays a more important role than impact energy dissipation. Larger impact vibrator (mass/moment of inertia) and smaller impact recovery coefficient are more beneficial to vibration suppression. Meanwhile, the vibrations generated by robotic drilling are effectively suppressed by the proposed semi-active vibration control under different frequency and amplitude excitation conditions.

References

[1] SCHNEIDER U, DRUST M, ANSALONI M, et al. Improving robotic machining accuracy through experimental error investigation and modular compensation [J]. The International Journal of Advanced Manufacturing Technology, 2016, 85(1): 3-15.
[2] LI C, WANG Z Q, KANG Y G, et al. Modal analysis of bracket structure in automatic drill-riveting system based on ABAQUS[C]//International Conference on Machinery. Hangzhou: Atlantis Press, 2016: 627-631.
[3] SEIFEDDINE M, VINCENT G, THIEN P L, et al. Dynamic characterization of machining robot and stability analysis[J]. The International Journal of Advanced Manufacturing Technology, 2016, 82(1): 351-359.
[4] WANG D. Analysis of vibration energy dissipation with vibro-impact absorber[J]. Journal of Mechanical Engineering, 2014, 50(17): 87-92.
[5] LI J W, ZHAO Z F. Vibration reduce for an impact damper coupled with nonlinear energy sink[J]. Journal of Dynamics and Control, 2020, 8(2):76-81. (In Chinese)
[6] GENG X F, DING H, WEI K X, et al. Suppression of multiple modal resonances of a cantilever beam by an impact damper[J]. Applied Mathematics and Mechanics, 2020, 41(3): 383-400.
[7] LI S J, YANG W T, DU Z K, et al. Study on a pounding tuned rotary mass damper and its vibration reduction performance[J]. Journal of Vibration Engineering, 2018, 31(5): 845-853. (In Chinese)
[8] LI S J, SUN L, YU H, et al. Experimental study on the vibration control performance of a pounding tuned rotary mass damper [J]. Journal of Vibration Engineering, 2020, 33(5): 861-868. (In Chinese)
[9] KONG F, XIA H B, SUNC, et al. Pounding tuned mass damper for vibration control of offshore wind turbine subjected to combined wind and wave excitations[J]. Journal of Vibration and Shock, 2021, 40(3): 19-27. (In Chinese)
[10] YANG Z C, LI Z J. Design and test for a type of particle impact damped dynamic absorber[J]. Journal of Vibration and Shock, 2010,29(6):69-71,143,236. (In Chinese)
[11] HUA C C, CHEN J Q, CHEN J N, et al. Adaptive prescribed performance control for torsional vibration of cold rolling mill with disturbance uncertainties[J]. Journal of Mechanical Engineering, 2021, 57(4): 202-209.
[12] GAO P, LIU H, XIANG C L, et al. Study on torsional isolator and absorber comprehensive vibration reduction technology for vehicle powertrain[J]. Journal of Mechanical Engineering, 2021, 57(14): 244-252.
[13] HARIS A, ALEVRAS P, MOHAMMADPOUR M, et al. Design and validation of a nonlinear vibration absorber to attenuate torsional oscillations of propulsion systems[J]. Nonlinear Dynamics, 2020, 100(1): 33-49.
[14] XU J W, YANG X F, LI W, et al. Design of quasi-zero stiffness joint actuator and research on vibration isolation performance[J]. Journal of Sound and Vibration, 2020, 479: 115367.
[15] ZHANG L X, ZHAO C M, QIAN F, et al. A variable parameter ambient vibration control method based on quasi-zero stiffness in robotic drilling systems[J]. Machines, 2021, 9(3): 67.
[16] ZHANG L X, ZHAO C M, QIANF, et al. An active control with a magnetorheological damper for ambient vibration[J]. Machines, 2022, 10(2): 82.
[17] BIAN Y S, GAO Z H, HU J T, et al. A semi-active control method for decreasing longitudinal torsional vibration of vehicle engine system: theory and experiments [J]. Journal of Sound and Vibration, 2019, 439: 413-433.
[18] WANG D, LEE Y S, McFARLAND D M, et al. Mitigating the effect of impact loading on a vehicle using an essentially nonlinear absorber[J]. Vehicle System Dynamics, 2009, 47(10): 1183-1204.

ZHANG Laixi, born in 1973. He received his Ph. D degree in mechanical and electronical engineering from School of Mechanical Engineering, Southeast University, Nanjing, China, in 2013. He is currently an associate professor in School of Mechanical and Electronical Engineering, Lanzhou University of Technology, Lanzhou, China. His research interests include high precision motion control, kinematics and dynamics of machinery, machine tools, robotics, and error compensation for machine tools.